Survey Review, **43**, 323 pp. 472-483 (October 2011)

ON CONSTRAINING ZENITH TROPOSPHERIC DELAYS IN PROCESSING OF LOCAL GPS NETWORKS WITH BERNESE SOFTWARE

P. Wielgosz, J. Paziewski and R. Baryła

University of Warmia and Mazury in Olsztyn,
Oczapowskiego 1, Olsztyn, Poland

ABSTRACT

The aim of this research was to develop the best strategy for the mitigation of the tropospheric delays in processing of precise local GPS networks. With the requirement of sub-centimetre accuracy and the availability of precise IGS products, one of the ultimate accuracy limiting factors in GPS positioning is the tropospheric delay. This is especially true for the accuracy of the height component. In many precise GPS applications, e.g. ground deformation and displacement analyses, volcano monitoring, the vertical accuracy is of crucial importance.

Several processing strategies for the troposphere modelling available in the Bernese software were applied and tested. The results from our research show that in the case of small networks (with baselines <10 km and point height differences < 100m)the best strategy is to use of a troposphere model in order to derive zenith tropospheric delays that are fixed in the adjustment. This allows to achieve mm-level accuracies of both horizontal and vertical coordinates. The estimation of the tropospheric delays from the GPS data does not provide satisfactory results, even in the case of a relative troposphere estimation.

KEY WORDS**:** GPS. Satellite networks. Precise positioning. Zenith tropospheric delay

INTRODUCTION

The influence of the neutral atmosphere on GNSS (Global Navigation Satellite System) signals is commonly called the tropospheric delay. It is an important element which diminishes the accuracy of GNSS measurements and causes systematic biases. As it is strongly correlated with the estimated height, the tropospheric delay predominately affects the accuracy of the height coordinate component rather than the horizontal components [**20**]. Nowadays, it is believed that in GNSS precise positioning the ultimate accuracy-limiting factor is the tropospheric delay [**20**], [**5**], [**10**]. Yet, a millimetre-level accuracy in the vertical coordinate is often required. In many precise GNSS surveying applications, e.g. ground deformation, displacement analyses, volcano monitoring, the vertical accuracy is of great importance. Hence, the mitigation of the tropospheric delays is crucial to the processing of local GNSS networks and still a hot topic for Earth sciences and geodetic and surveying applications. However, one must also take care of the other error sources such as ionospheric delays, multipath effects and signal obstructions.

With respect to the water vapour content, it is common to divide the troposphere into two parts: a hydrostatic and a non-hydrostatic part, sometimes called dry and wet part, respectively. It is agreed that about 90% of the tropospheric delay is caused by the dry part of the troposphere [**13**]. The total tropospheric delay in the zenith direction amounts to about 2.4 m at sea level. Tropospheric zenith delay models for hydrostatic

Contact: P Wielgosz e-mail: pawel.wielgosz@uwm.edu.pl

  DOI 10.1179/003962611X13117748891877

and non-hydrostatic components are functions of meteorological parameters. It is not difficult to compute the hydrostatic part of the tropospheric delay. It may be calculated from various hydrostatic tropospheric models that use standard atmospheric parameters, surface meteorological measurements or using parameters obtained from models like GPT (Global Pressure and Temperature), which do not require external input data, or from numerical weather models like ECMWF (European Centre for Medium-Range Weather Forecasts) [**4**]. On the other hand, it is extremely difficult to model or determine the distribution of the water vapour, which is crucial for the ability to correct the non-hydrostatic delay, because its distribution is neither linear nor homogenous, and varies in the horizontal and vertical plane [**26**], [**23**].

The tropospheric delay to a satellite observed at a particular elevation angle is called the slant total tropospheric delay (STD). In the most straightforward representation of GNSS signals, each satellite's signal has its own STD: a complex equation, because there are usually many satellites visible at every epoch. Fortunately, it is a reasonable approximation (and numerically advantageous) to assume that the STD can be created from the zenith total delay (ZTD). The tropospheric delay towards the zenith above the antenna has, by definition, no elevation dependence and would be the same for all observations at an epoch. The STD is obtained by multiplying the ZTD with a mapping function. Mapping functions are mathematical formulas that account for the elevation angle and allow to convert a ZTD to the appropriate STD [**14**], [**18**], [**25**]. Mapping functions, like tropospheric models, depend on meteorological parameters. They have already been compared by several researchers [**30**], [**5**]; however, those studies concern rather large (global) scale networks. The STD for any satellite at any elevation angle can be computed from [**15**]:

$$STD(E) = ZHD \times m_d(E) + ZWD \times m_w(E) \tag{1}$$

where:
E - elevation angle,
$STD(E)$ - slant total delay,
ZHD - zenith hydrostatic (dry) delay
$m_d(E)$ - mapping function for the hydrostatic part,
ZWD - zenith non-hydrostatic (wet) delay,
$m_w(E)$ - mapping function for the non-hydrostatic part.

There are several methods of mitigating the tropospheric delay in precise, relative GNSS positioning [**2**], [**10**]. The easiest way is to assume that the tropospheric delay is the same (or very similar) on both ends of a baseline. This is true only for short baselines with very small height differences, where this bias is (mostly) reduced by double differencing of the original observations. Another possibility is to use tropospheric models in the processing, for example Saastamoinen, Hopfield and Modified Hopfield with standard atmosphere parameters [**11**], [**17**], [**13**], [**15**]. A slightly different approach is to use these models with surface meteorological data collected at the observation sites or obtained from global or regional numerical meteorological models like ECMWF, COAMPS (Coupled Ocean/Atmosphere Mesoscale Prediction System) or simplified models like GPT [**4**]. Research shows that meteorological parameters derived in these two ways show reasonable agreement [**7**], [**1**]. The most advanced method is to treat the tropospheric delay as a parameter in the least squares adjustment and to estimate it in the post-processing of the GNSS data, using ZHD or ZTD from tropospheric models only as *a priori* information. This,

however, requires the processing of long baselines (over 100 km), due to the correlation of the ZTD at close sites. When processing small, precise networks, a relative modelling is recommended [**10**], [**29**]. In this strategy, the model-derived ZTD for one (or more) stations is fixed or tightly constrained. The corrections for all other sites are allowed to change. This results in corrections for all other sites relative to the fixed ZTD at the selected site.

Studies on the mitigation of the tropospheric delay in precise surveying applications like deformation monitoring have been carried out by several research groups. Published results concerned volcano monitoring with very large height differences between the control points [**22**], open pit mines monitoring [**6**], geodynamic studies [**8**], dam structural monitoring [**24**] and many others. The latest studies concern applications of mapping functions derived from numerical weather models, like GMF (Global Mapping Function) and VMF1 (Vienna Mapping Function), to GPS processing [**3**]. These mapping functions are said to provide the most accurate troposphere modelling today [**25**]. However, the dependence of the VMF1 on external data can be a drawback.

The study presented here concerns an urban area. The analyses were carried out using the Bernese v. 5.0 GPS software, which is very often used in geodynamics studies and high-precision deformation monitoring [**10**]. The Bernese software was primarily designed for the processing of large-scale GNSS networks. This application is well studied and documented in the literature [**9**]. However, a processing strategy for precise local networks is not evaluated completely. This mostly concerns the proper treatment of the tropospheric delays. The aim of this research was to study the influence of the different strategies of the tropospheric delay mitigation available in the Bernese software on the resulting coordinate accuracy in local, precise satellite networks (with baselines of less than about 10 km). The main focus of this study was to assess the proper level of the constraints imposed on ZTD parameters in the adjustment.

EXPERIMENT

The test area is located in the Main and Old City of Gdansk in Poland. This network was established earlier for precise ground deformation monitoring. The network consists of 4 reference points (PP) and 12 monitoring points (CC). Two main reference points (PP02 and PP05) were used in this experiment. Their known coordinates were constrained to 0.002 m. Two secondary reference points (PP03 and PP04) are routinely used only to check the stability of the main points. The length of the processed baselines varied from 1.0 km to 3.2 km. The monuments of the reference points were established in a stable area, at ellipsoidal heights of approximately 75-95 m. The monitoring points were located at heights of 30-36 m. Thus the average height difference between the monitoring and the reference points is about 60 m. The geoidal undulation in this region is approximately 30 m. It should be emphasized that the GPS antennas at the reference points were mounted on concrete pillars by means of forced centring. The antennas were removed between the sessions and mounted again at the beginning of the next session. Their heights above the pillar benchmarks were precisely measured with precision of 0.1 mm. At the monitoring points, the antennas were mounted using special metal poles that provided forced centring. This solution does not allow any changes of the antenna position (including its height over a point) between the observational sessions of the campaign. Please note that mounting GPS antennas on tripods (instead of using forced centring on pillars or metal poles) may not deliver the accuracy as presented here. Also it should be noted that all the monitoring

points were located in a difficult environment where urban canyons limit the satellite visibility at low elevation angles.

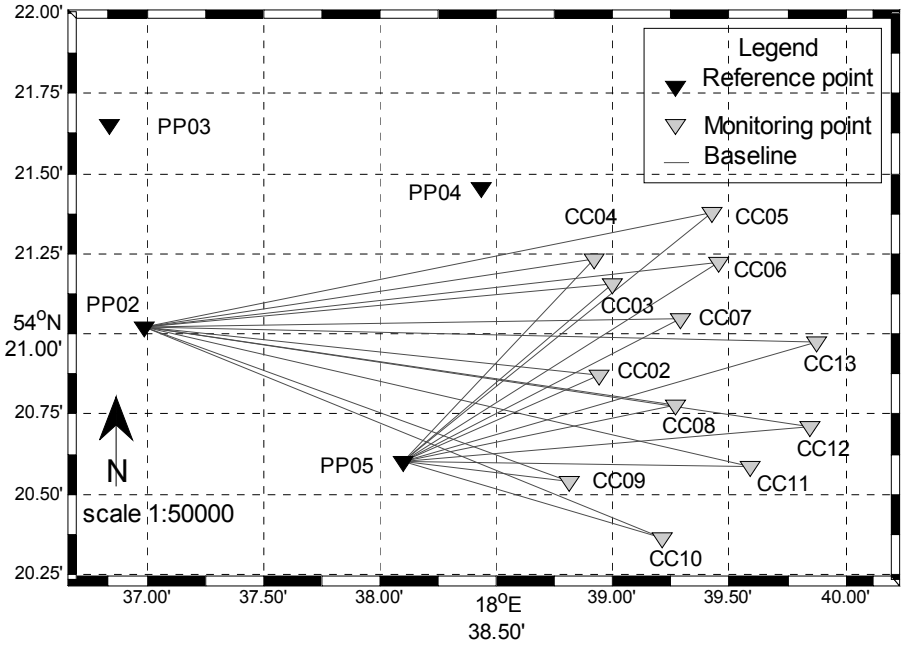

Fig. 1. Test network for deformation monitoring

The coordinates of the reference sites were previously determined in the ITRF2005 (International Terrestrial Reference Frame) reference frame by processing long baselines to the neighbouring IGS (International GNSS Service) stations using data from six 8-hour long sessions carried out during daytime. The observations at each monitoring point were carried out over 3 days (every second day of the campaign, 8-hour long sessions). Thus three independent position solutions of each monitoring site were obtained. The whole campaign lasted 6 days. The Bernese 5.0 GPS software was used for the processing of the collected data. The computations were carried out using L1 carrier-phase observations. In order to obtain the highest possible precision, the IGS final satellite orbits, earth rotation parameters and absolute antenna phase centre variations and offsets were used. In addition, a regional ionosphere model from the Centre of Orbit Determination in Europe (CODE) was used in order to remove residual ionospheric delays [**21**]. The SIGMA method was applied for the ambiguity resolution [**10**]. Only independent, manually chosen, and simultaneously observed baselines were processed (network solution, Figure 1). The elevation cut-off was set to 10 degrees. Low elevation angles generally help to estimate the ZTD because of a better discrimination between the estimated height, clock correction and tropospheric delay [**20**]. On the other hand the trade-off is a poorer signal-to-noise ratio and increased numbers of cycle slips, increased multipath, etc. However, the urban environment did not allow to collect data at elevations lower than 10 degrees. It should be noted that for two locations the obstructions limited satellite visibility to elevations over 20 degrees (CC09) and over 30 degrees (CC07).

There is a wide choice of tropospheric delay models and mapping functions, as mentioned above. Here, only the processing strategies with different approaches for the reduction of the tropospheric delay available in the Bernese software were examined.

The main analyses concerned testing different levels of the constraints (tight and loose) imposed on the estimated ZTD parameters (Table 1). In addition, this allowed to assess the possibility of a relative estimation of the ZTD in local networks.

Table 1. *Processing strategies*

Strategy	*A priori troposphere modelling (model + mapping function)*	*Site specific parameters (mapping function for estimated part)*	*ZTD constraints for*	
			Reference sites PP	*Monitoring sites CC*
1	No tropospheric corrections			
2	Dry Saastamoinen + Dry Niell	-	fixed	fixed
3a	Saastamoinen + Dry Niell	Wet Niell	fixed	0.1 mm
3b	Saastamoinen + Dry Niell	Wet Niell	fixed	1 mm
3c	Saastamoinen + Dry Niell	Wet Niell	fixed	10 mm
3d	Saastamoinen + Dry Niell	Wet Niell	fixed	100 mm
4	Modified Hopfield model with surface meteorological data	Wet & Dry Niell	fixed	fixed

Strategy 1: No tropospheric corrections were applied, hence neglecting completely the influence of the troposphere on GPS measurements. This strategy is evaluated for comparison only.

Strategy 2: Only the hydrostatic delays were calculated (from the Saastamoinen model) and used to correct the GPS observables, neglecting the influence of the non-hydrostatic (wet) part. This strategy is also evaluated for comparison only.

Strategy 3: Relative ZTD modelling was applied. The ZTDs for two reference points (PP02 and PP05) were obtained from the Saastamoinen model and fixed in the adjustment. The a priori ZTD values for the monitoring points were also obtained from the Saastamoinen model. However, these values were constrained in the adjustment using a different level of constraints in order to analyse their influence on the results. Hence, four versions of the strategy 3 were derived:

3a) with constraints of 0.1 mm imposed on the a priori ZTDs for the monitoring sites (effectively fixing the ZTDs to their a priori values),
3b) with constraints of 1.0 mm,
3c) with constraints of 10.0 mm,
3d) with constraints of 100.0 mm.

The interval between the estimated subsequent ZTD parameters was one hour. The Wet Niell mapping function was used for the computation of the partial derivatives of the troposphere zenith delay parameters [**18**]. This strategy was expected to provide the best results.

Strategy 4: The ZTDs were obtained from an external source and used to correct the GPS observables in the processing. Here, the ZTDs were computed using the Modified Hopfield model [**11**], [**31**] entering real meteorological data from a nearby meteorological station. All computations were carried out without estimating a troposphere gradient. The summary of the processing strategies is presented in Table 1.

RESULTS

The sample ZTDs obtained from the different processing strategies on the first day of the experiment (9 June 2008) are presented in the Figures 2 and 3. Figure 2 shows an example of the atmospheric parameters observed at a nearby meteorological station on that day. The temperature ranged from 296.0 K to 299.2 K. The pressure and the relative humidity were also rather stable on that day.

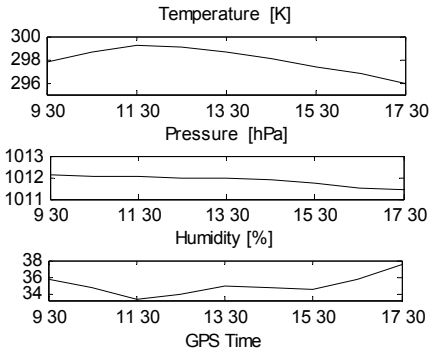

Fig. 2. Troposphere parameters observed during the experiment at a nearby meteorological station, 9 June 2008 (Local Time = GPS Time + 2 hours)

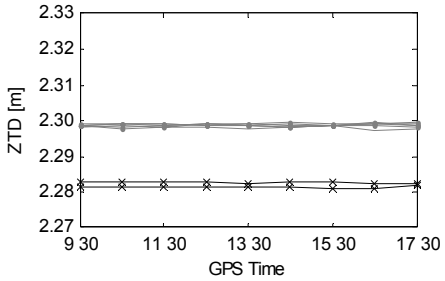

Fig. 3. ZTD, strategy 2, 9 June 2008

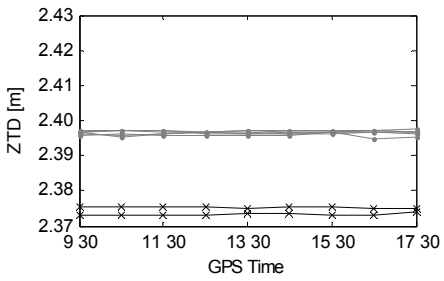

Fig. 4. ZTD, strategy 3a, 9 June 2008

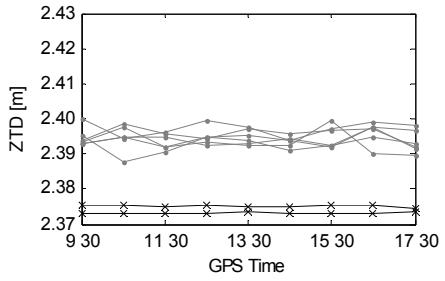

Fig. 5. ZTD, strategy 3d, 9 June 2008

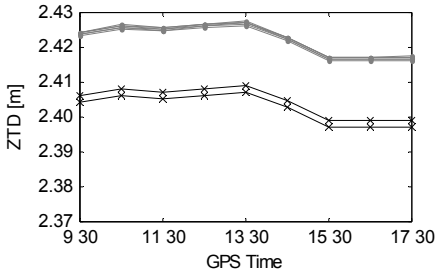

Fig. 6. ZTD computed from meteorological data using Modified Hopfield model, strategy 4, 9 June 2008

Figures 3-6 show the ZTDs obtained for the processed points. The ZTDs for the reference sites are marked with black lines with crosses, and ZTDs for the monitoring points are marked with light grey lines with dots. There is no need to distinguish

between particular monitoring points here. It can be clearly seen that the ZTD for the reference sites is usually ~ 2 cm lower than the one for the monitoring sites. This effect concerns all strategies and is due to the height difference of ~ 60 m between these sites.

Figures 3-5 illustrate that there is a systematic shift of about 10 cm between the tropospheric delays obtained from the Strategies 2 and 3. This is due to the omission of the wet delay in the Strategy 2. Figure 5 shows that the tropospheric delays estimated when using Strategy 3d with loose constraints vary (± 1 cm) not only between the subsequent epochs, but also between the neighbouring sites. However, the tropospheric conditions over the entire network were very similar and such variations are rather unrealistic. This indicates that the quality of the ZTD obtained with 3d is rather poor. In the Strategy 3a with fixed constraints all monitoring points received very similar ZTDs. The ZTDs obtained from the meteorological data (Figure 6) confirms that these parameters should be very similar at the neighbouring stations (as in the Strategy 3a). However, they show some variations during the session. Of course, this feature is not reflected in the results of the Strategy 3a. The ZTD values obtained with the Modified Hopfield model with meteorological data (4) are usually about 2.5 cm higher that the ones obtained from the Saastamoinen model (3a) with standard atmosphere parameters.

Table 2. *Differences between the minimum and maximum values of ZTD at monitoring points obtained from different strategies*

Strategy		***2***	***3a***	***3b***	***3c***	***3d***	***4***
		[mm]	*[mm]*	*[mm]*	*[mm]*	*[mm]*	*[mm]*
Session	9 June 2008	2.02	2.42	9.97	10.81	10.82	1.95
	10 June 2008	2.04	2.65	18.38	41.11	41.68	2.05
	11 June 2008	2.06	2.31	17.00	19.86	19.90	2.00
	12 June 2008	2.24	2.81	18.09	37.85	38.20	2.01
	13 June 2008	2.48	2.90	12.23	14.67	14.17	2.04
	14 June 2008	1.90	2.77	15.14	21.44	21.49	2.07

Table 2 gives the differences between the minimum and maximum ZTDs obtained for the monitoring points for selected processing strategies for all days of the campaign. It should be noted that the monitoring points are located within a small area with small height differences (from 0.8 m to 7.1 m above sea level). It is expected that in such cases the ZTD parameters should be very similar. The results obtained when using the strategy 3d with loose constraints on the ZTD parameters and the Strategy 3c show the greatest variations (about 4.2 cm). Introducing relatively tight constraints (1mm) on the ZTD parameter in the strategy 3b still resulted in a great diversity of the estimated ZTD, up to 1.8 cm. The ZTD parameters computed with the Strategies 2 and 3a (with fixed constraints) and the Strategy 4 are similar with low variability (> 0.3 cm), as may be expected in such small networks.

Another analysis presented here concerns the influence of the different strategies on the carrier phase ambiguity resolution and the coordinates' repeatability (Tables 3, 4 and 5). The figures presented in Table 3 indicate that all the tested strategies resulted in equally high success rates for a correct ambiguity resolution. This means that the troposphere modelling has an insignificant impact on the ambiguity resolution when processing small networks.

Table 3. *Average percentage of the correctly resolved ambiguities for different processing strategies*

Strategy	***1***	***2***	***3a***	***3b***	***3c***	***3d***	***4***
	[%]	*[%]*	*[%]*	*[%]*	*[%]*	*[%]*	*[%]*
Average % of the resolved ambiguities	96.7	98.4	98.3	98.1	98.2	98.2	98.4

Table 4. *Average coordinate repeatability at monitoring points with respect to the applied processing strategy*

Strategy		*1*	*2*	*3a*	*3b*	*3c*	*3d*	*4*
		[mm]	*[mm]*	*[mm]*	*[mm]*	*[mm]*	*[mm]*	*[mm]*
Coordinate component	*N*	1.0	1.0	1.0	1.0	1.0	1.0	1.0
	E	0.9	0.9	0.9	0.8	0.8	0.8	0.9
	H	**1.5**	**1.0**	**1.0**	**2.8**	**4.4**	**4.5**	**1.0**

Table 4 presents average repeatability of the obtained coordinate components of the monitoring points for all presented strategies. A standard deviation (dispersion) of the coordinate components obtained from the results of the independent processing of three observation sessions served here as a measure of the repeatability. This standard deviation is the variation of the differences about the mean difference. The average repeatability of the height component (H) for the strategies with loose constraints on the estimated ZTD (3c and 3d) is definitely worse than for the Strategies 1, 2, 3a, 3b and 4 with tight or fixed constraints (no estimation). Table 4 also indicates that the strategy selection almost did not affect the repeatability of the horizontal components.

Table 5. *Differences between the obtained ellipsoidal heights with respect to the Strategy 3a*

Site	h_{3a}-h_1	h_{3a}-h_2	h_{3a}-h_{3b}	h_{3a}-h_{3c}	h_{3a}-h_{3d}	h_{3a}-h_4
	[mm]	*[mm]*	*[mm]*	*[mm]*	*[mm]*	*[mm]*
PP02	1.6	0.5	-0.1	-0.1	-0.1	0.1
PP05	-1.5	-0.5	0.1	0.2	0.2	-0.1
CC02	-52.4	-13.2	-4.2	-5.8	-5.8	-5.2
CC03	-49.5	-12.8	-2.3	-2.5	-2.5	-5.1
CC04	-47.5	-12.4	0.6	0.1	0.2	-5.0
CC05	-51.3	-13.1	-4.8	-6.3	-6.3	-4.8
CC06	-51.9	-13.6	1.3	4.8	4.9	-5.6
CC07	-46.7	-12.2	-5.7	-15.7	-16.0	-4.5
CC08	-53.3	-13.8	-8.2	-10.7	-10.7	-5.1
CC09	-52.2	-13.3	4.0	5.0	4.7	-5.9
CC10	-54.7	-14.0	-2.4	-3.7	-3.7	-5.9
CC11	-52.5	-13.6	-2.0	-3.5	-3.7	-5.7
CC12	-53.8	-13.8	-4.6	-6.7	-6.6	-5.5
CC13	-52.3	-13.6	2.8	3.4	3.5	-5.8

The following analyses compare the ellipsoidal heights obtained with different troposphere modelling strategies. These clearly show the impact of the applied strategy. Table 5 presents the differences between the ellipsoidal heights obtained using each of the tested strategies with respect to the results of the Strategy 3a (see Table 1) used as a reference. The results from Table 5 show that Strategy 4 presents constant bias of ~5 mm and 3b shows rather random distribution of the residuals

(ranging from -8.2 to +4.0 mm). The results show a systematic shift between the heights of the monitoring points ranging from about 5 mm (Strategy 4) to 50 mm (Strategy 1). This shift is caused by the height differences between the reference and the monitoring points, which clearly affects the results obtained with the tested strategies.

The neglect of the tropospheric delays produces a very large bias of about 50 mm (Strategy 1) in relation to the reference Strategy 3a. Neglecting the non-hydrostatic delays (Strategy 2) results in smaller bias of about 13 mm. The results obtained with the strategies that allow, to some extent, to estimate the ZTD (3b-3d) show random differences. The looser the constraints the more random the differences are. Basically, this means that due to the strong correlations between the ZTDs in small local networks, these parameters cannot be reliably estimated. The solution with the fixed ZTD obtained from the meteorological data (4) produces heights that are shifted by about 5 mm. This solution is the closest to the Strategy 3a. Also, the above and the results from Tables 4 and 6 gave us reasons to believe that Strategy 4 is better than 3b and may be considered as good as 3a.

The strategies can be also verified by comparing the height differences between the processed sites derived from GPS with the use of the quasigeoid model ($\Delta H_{n\ SAT}$) to the height differences obtained from precise, geometric levelling (ΔH_n) (called precise levelling below). The normal heights (commonly known as ortometric heights, for definition see [**17**], [**27**], p.372) derived from the GPS levelling were computed from a well known formula [**27**], [**12**]:

$$H_{n\ SAT} = h - \xi \tag{2}$$

where:

$H_{n\ SAT}$ – normal height obtained from GPS levelling,

h – ellipsoidal height from GPS,

ξ – height anomaly (quasigeoid - ellipsoid separation).

The height anomalies were interpolated from the regional model of the quasigeoid for Poland [**19**]. Since the height differences ΔH_n are the observed quantities in precise geometric levelling, they should be compared to the corresponding quantities obtained from GPS levelling ($\Delta H_{n\ SAT}$). This comparison can be considered as an indicator of the relative bias of the satellite levelling (because the accuracy of the precise levelling is expected to be much better). This comparison is not contaminated by the absolute bias of the quasigeoid model. Table 6 lists the averages of the absolute differences between the adjusted height differences from precise geometric levelling and the satellite levelling. The best consistency was observed for the Strategies 3a and 4 (both with fixed tropospheric delays). Again, the worst results come from the strategies with constraints on the estimated ZTD (3c and 3d) and from the Strategy 1 with no tropospheric correction.

Table 6. *Average differences between normal height differences obtained from precise and satellite levelling and their standard deviations*

Strategy	*1*	*2*	*3a*	*3b*	*3c*	*3d*	*4*
	[mm]	*[mm]*	*[mm]*	*[mm]*	*[mm]*	*[mm]*	*[mm]*
AVERAGE	12.2	7.6	**6.6**	8.2	10.5	10.5	**6.7**
STD	16.1	7.3	**7.6**	9.3	12.8	12.9	**7.3**

Table 7 shows a detailed comparison of the height differences for the Strategy 3a. This strategy expresses the smallest differences between the height differences obtained from classical precise levelling and satellite levelling. The differences are usually smaller than 10 mm. Please note that the worst results (larger than 10 mm) were obtained for baselines that include the monitoring points CC07 and CC09 that are located in difficult GPS environment.

Table 7. *Normal height differences obtained from precise and satellite levelling (Strategy 3a)*

Height difference	ΔH_n	$\Delta H_{n\,SAT}$	$\Delta H_n - \Delta H_{n\,SAT}$
	[m]	*[m]*	*[mm]*
*PP05-**CC09***	-55.5799	-55.5779	**-2.0**
***CC09**-CC10*	-1.5678	-1.5802	**12.4**
CC10-CC11	-0.3846	-0.3847	0.1
CC11-CC12	-0.2293	-0.2290	-0.3
CC12-CC13	0.0227	0.0245	-1.8
CC13-CC08	1.5562	1.5637	-7.5
CC08-CC02	1.8482	1.8376	10.6
CC03-CC02	-0.8638	-0.8641	0.3
CC03-CC04	1.9786	1.9850	-6.4
CC04-CC05	-4.6044	-4.6070	2.6
CC05-CC06	0.7595	0.7531	6.4
***CC07**-CC06*	-0.7181	-0.7462	**28.1**
*CC08-**CC07***	1.5638	1.5790	**-15.2**
PP05-PP02	6.029	6.0276	1.4
PP02-CC04	-57.5211	-57.5245	3.4

CONCLUSIONS

It was shown that the troposphere modelling in small precise networks mainly influences the obtained height component. It shows negligible effect on the horizontal components of the site coordinates. The best results are obtained by fixing ZTD in the adjustment (Strategies 3a and 4) derived from tropospheric models (Saastamoinen, Modified Hopfield or any other). Therefore, it is not recommended to estimate the tropospheric delays (even the relative corrections) in networks with short baselines and relatively small height differences, but rather to apply and fix ZTD obtained from troposphere models. This was proved by the comparison to the precise geometric levelling.

Setting relatively loose constraints on ZTD (strategies 3c and 3d) results in large ZTD discrepancies between close points at similar heights (which is rather unrealistic) and, consequently, provides worse height estimations. Even setting tight constraints of 1 mm (Strategy 3b) gives lower accuracy results compared to fixed solutions (Strategy 3a and 4).

The selected strategy does not have any noticeable impact on the ambiguity resolution. We recommend the Strategies 3a and 4, since they take into account the full tropospheric delay and show good results in comparison to precise levelling. These strategies are the most suitable for precise surveying applications, such as deformation monitoring in small precise satellite networks processed with the Bernese software.

ACKNOWLEDGEMENTS

These studies were supported by grant from Polish Ministry of Science and Higher Education no N526 251938. The authors are grateful to the Chair of Satellite Geodesy and Navigation UWM for collecting the GPS data used in the experiments. Meteorological data used in this publication were made available free of charge and remain ownership of Fundacja Agencji Regionalnego Monitoringu Atmosfery Aglomeracji Gdańskiej ARMAAG.

References

1. Andrei, C. O., Chen, R., 2009. Assessment of time-series of troposphere zenith delays derived from the Global Data Assimilation System numerical weather model. *GPS Solutions* 13:109-117.
2. Bock, O., Doerflinger, E., 2001. Atmospheric modeling in GPS data analysis for high accuracy positioning, *Phys. Chem. Earth* (A), 26, (6-8): 373-383.
3. Boehm, J., Werl, B., Schuh, H., 2006. Troposphere mapping functions for GPS and very long baseline interferometry from European Centre for Medium-Range Weather Forecasts operational analysis data. *J Geophys Res,* 111:B02406.
4. Boehm, J., Heinkelmann, R., Schuh, H., 2007a. Short note: a global model of pressure and temperature for geodetic applications. *J Geod,* 81(10):679-683.
5. Boehm, J., Mendes Cerveira, P. J., Schuh, H., Tregoning, P., 2007b. The impact of tropospheric mapping functions based on numerical weather models on the determination of geodetic parameters. In: Tregoning P, Rizos C. (eds) *Dynamic planet-monitoring and understanding a dynamic planet with geodetic and oceanographic tools.* Springer, International Association of Geodesy Symposia, 130:837-843.
6. Bond, D. J., 2007. *Bringing GPS into Harsh Environments for Deformation Monitoring. Ph.D. dissertation*, Department of Geodesy and Geomatics Engineering, Technical Report No.253, University of New Brunswick, Fredericton, New Brunswick, Canada.
7. Bosy, J., Borkowski, A., 2006. Troposphere modeling in local GPS network. *EUREF Publication No. 15, Mitteilungen des Bundesamtes für Kartographie und Geodäsie,* Vienna, Austria, June 1-4 2005, EUREF Publication No. 15, Mitteilungen des Bundesamtes für Kartographie und Geodäsie Band 38, pp. 356-362.
8. Bosy, J. Kontny, B., Borkowski, A., 2009. IGS/EPN reference frame realization in local GPS networks, H. Drewes (ed.), *Geodetic Reference Frames*, International Association of Geodesy Symposia 134, Springer-Verlag Berlin Heidelberg 2009, pp. 197-204
9. Bruyninx, C., 2007. Comparing GPS-only with GPS + GLONASS positioning in a regional permanent GNSS network. *GPS Solutions,* 11:97–106.
10. Dach, R., Hugentobler, U., Fridez, P., Meindl, M. 2007. Bernese GPS Software Version 5.0. Astronomical Institute University of Bern, Bern. 364 pages
11. Goad, C. C., Goodman L., 1974. A Modified Hopfield Tropospheric Refraction Correction Model. American Geophysical Union Annual Fall Meeting, San Francisco, California, December 12–17, pp. 28.
12. Hofmann – Wellenhof, B., Moritz, H., 2005. *Physical Geodesy*. Springer-Verlag, Wien. 404 pages
13. Hofmann – Wellenhof, B., Lichtenegger, H., Wasle, E., 2008. *GNSS – Global Navigation Satellite Systems GPS, GLONASS, GALILEO and more*. Springer, Wien-New York. 516 pages.
14. Ifadis, I., 1986. The atmospheric delay of radio waves: modeling the elevation dependence on global scale. Technical Report 38L, School of Electrical and Computer Engineering, Chalmers University of Technology, Gothenburg.
15. Leick, A., 2004. *GPS Satellite surveying*. John Wiley&Sons, New Jersey. 474 pages.
16. Misra, P., Enge, P., 2006. *Global Positioning System. Signals, Measurements, and Performance,* 2nd ed. Ganga-Jamuna Press, USA. 569 pages.

17. Molodenskij, M. S., Eremeev V. F., Yurkina M. I., 1960. *Methods for study of the external gravitational field and figure of the earth.* Translated from Russian by Israel Program for Scientific Translations for the Office of Technical Services, U.S. Department of Commerce, Washington, D.C., U.S.A., 1962
18. Niell, A. E., 1996. Global mapping functions for the atmosphere delay at radio wavelengths. *J Geophys Res,* 101(B2):3227-3246.
19. Pażus, R., Osada, E., Olejnik, S., 2002. Leveling Geoid 2001. *Geodeta*, No.5/2002 (in Polish).
20. Rothacher, M., 2002. Estimation of station heights with GPS. In: Drewes H, Dodson A, Fortes L, Sanchez L, Sandoval P (eds) *Vertical reference systems*. Springer, International Association of Geodesy Symposia, 124:81-90. 228 pages.
21. Schaer, S., 1999. *Mapping and Predicting the Earth's Ionosphere Using the Global Positioning System,* Ph.D. dissertation., Astronomical Institute University of Bern, Bern. 205 pages.
22. Schon, S., Wieser, A., Macheiner, K., 2005. Accurate tropospheric correction for local GPS monitoring networks with large height differences. In Proc. of ION ITM, 13-16 Sept. 2005, Long Beach, CA., pp. 250-260.
23. Schüler, T., 2001. *On ground-based GPS Tropospheric Delay Estimation*, Ph.D. dissertation. Universität der Bundeswehr. Munich. 364 pages.
24. Shaoquan, X., Jingnan, L., Zhenghan, L., Zhenhong, L., 2000. GPS automatic monitoring system for outside deformation of Geheyan Dam on the Qingjiang Rive. *Geo-Spatial Information Science*, Wuhan University of Technology, 3(2):58-64.
25. Steigenberger, P., Boehm, J., Tesmer, V., 2009. Comparison of GMF/GPT with VMF1/ECMWF and implications for atmospheric loading. *J Geod,* 83:943-951.
26. Teunissen, P. J. G., Kleusberg, A., 1998. *GPS for Geodesy*. Springer - Verlag. Berlin Heidelberg New York. 640 pages.
27. Torge, W., 1991. *Geodesy*. Walter de Gruyter, Berlin - New York. 234 pages.
28. Vanicek, P., Krakiwsky, E., 1986. *Geodesy: The Concepts*, 2nd ed. Amsterdam, Elsevier Science Publishers, 697 pages.
29. Wielgosz, P., Cellmer, S., Rzepecka, Z. and Grejner-Brzezinska D.A., 2008. Troposphere Modeling for Precise GPS Rapid-Static Positioning in Mountainous Areas, *Proceedings of the ION GNSS 2008*, September 16-19, Savannah, Georgia, pp. 634 – 638.
30. Vey, S., Dietrich, R., Fritsche, M., Rülke, A., Rothacher, M., Steigenberger, P., 2006. Influence of mapping functions parameters on global GPS network analyses: comparison between NMF and IMF. *Geophys Res Lett* 33:L01814.
31. Xu, G., 2007. *GPS, Theory, Algorithms and Applications*. Springer-Verlag. Potsdam. 340 pages.